Perivascular macrophages mediate microvasospasms after experimental subarachnoid hemorrhage

Xiangjiang Lin [1,4], Nicole A. Terpolilli MD[1,2,4], Julian Schwarting MD, B.Sc.[1-4] *, Nikolaus Plesnila MD, PhD[1,4] *

1 Institute for Stroke and Dementia Research (ISD), and
2 Department of Neurosurgery, Munich University Hospital,
Munich, Germany
3 Department of Diagnostic and Interventional Neuroradiology,
Klinikum rechts der Isar, Technische University Munich, Munich, Germany.
4 Munich Cluster for Systems Neurology (SyNergy), Munich, Germany

* These authors contributed equally

Correspondence to:
Nikolaus Plesnila, MD, PhD, Institute for Stroke and Dementia Research, University Hospital, LMU Munich, Feodor-Lynen Strasse 17, 81377 Munich, Germany.
nikolaus.plesnila@med.uni-muenchen.de

Running title: Perivascular macrophages mediate microvasospasms after subarachnoid hemorrhage

Total words: 3920

Figure 1

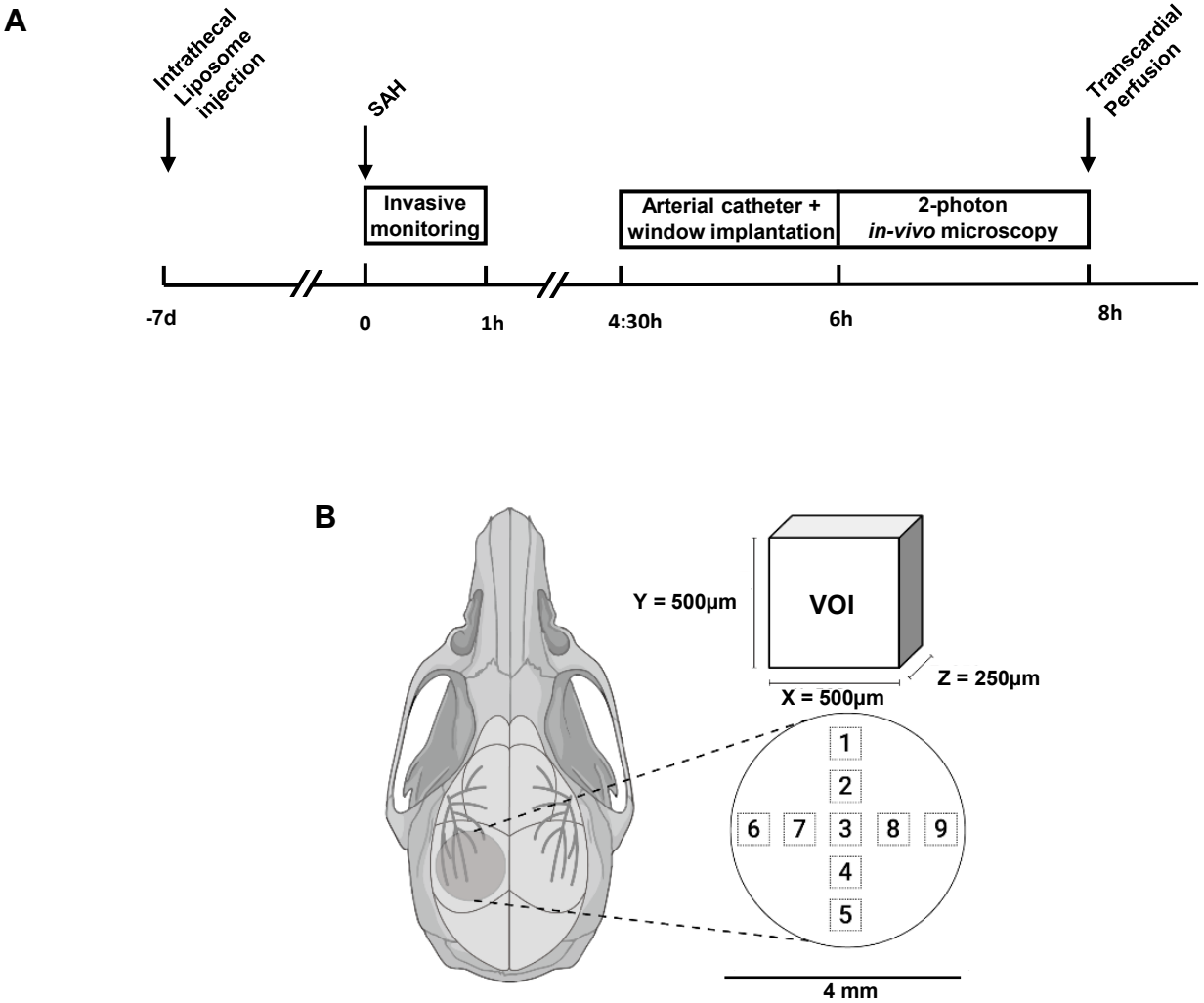
A
Intrathecal Liposome injection
SAH
Transcardial Perfusion
Invasive monitoring
Arterial catheter + window implantation
2-photon in-vivo microscopy
-7d
0
1h
4:30h
6h
8h
B
Y = 500µm
VOI
Z = 250µm
X = 500µm
1
2
6
7
3
8
9
4
5
4 mm
C
SAH
n=4-8
mean ±SD
Ipsilateral CBF (%baseline)
Contralateral CBF (%baseline)
time (min)
sham
SAH + vehicle
SAH + Clodronate

Figure 2

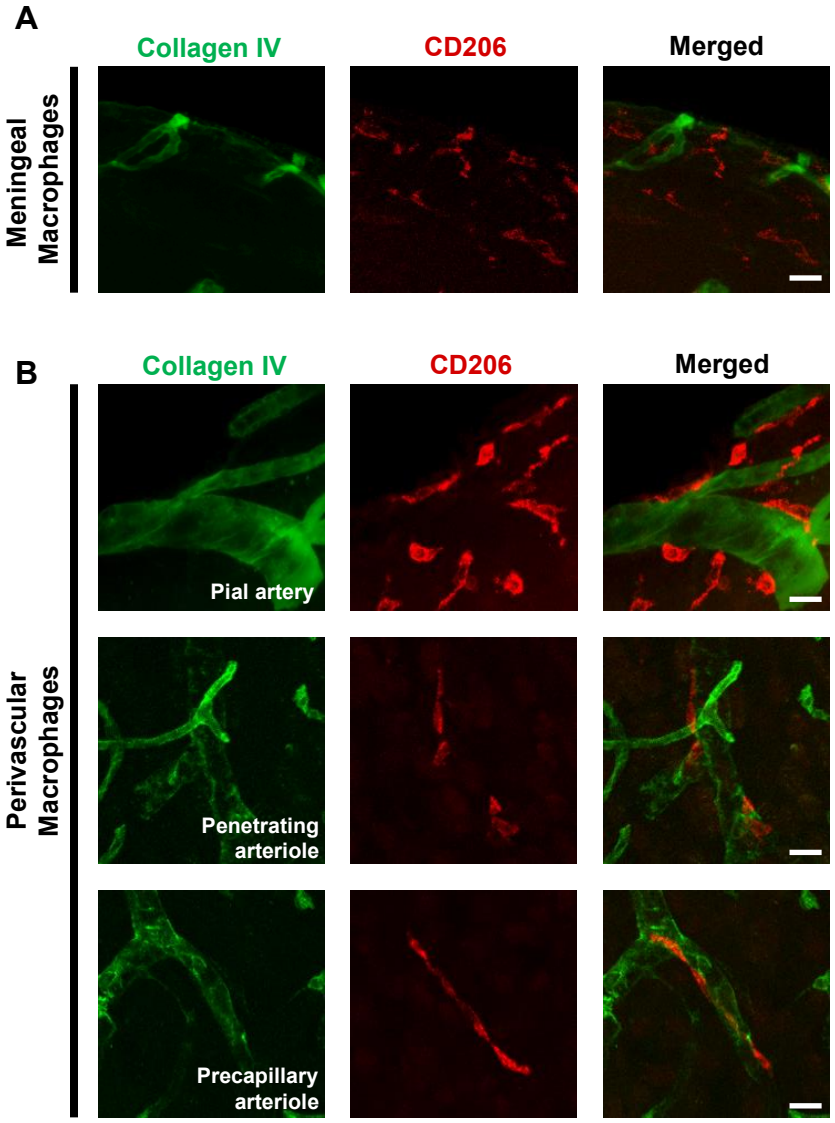
A
Collagen IV
CD206
Merged
Meningeal Macrophages
B
Collagen IV
CD206
Merged
Perivascular Macrophages
Pial artery
Penetrating arteriole
Precapillary arteriole

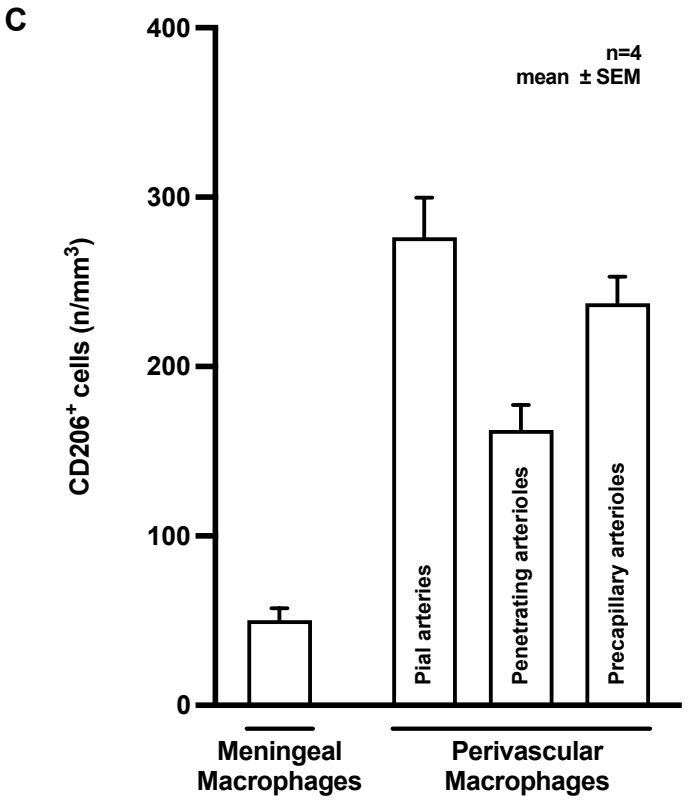
C
n=4
mean ± SEM
CD206+ cells (n/mm3)
400
300
200
100
0
Pial arteries
Penetrating arterioles
Precapillary arterioles
Meningeal Macrophages
Perivascular Macrophages

Figure 3

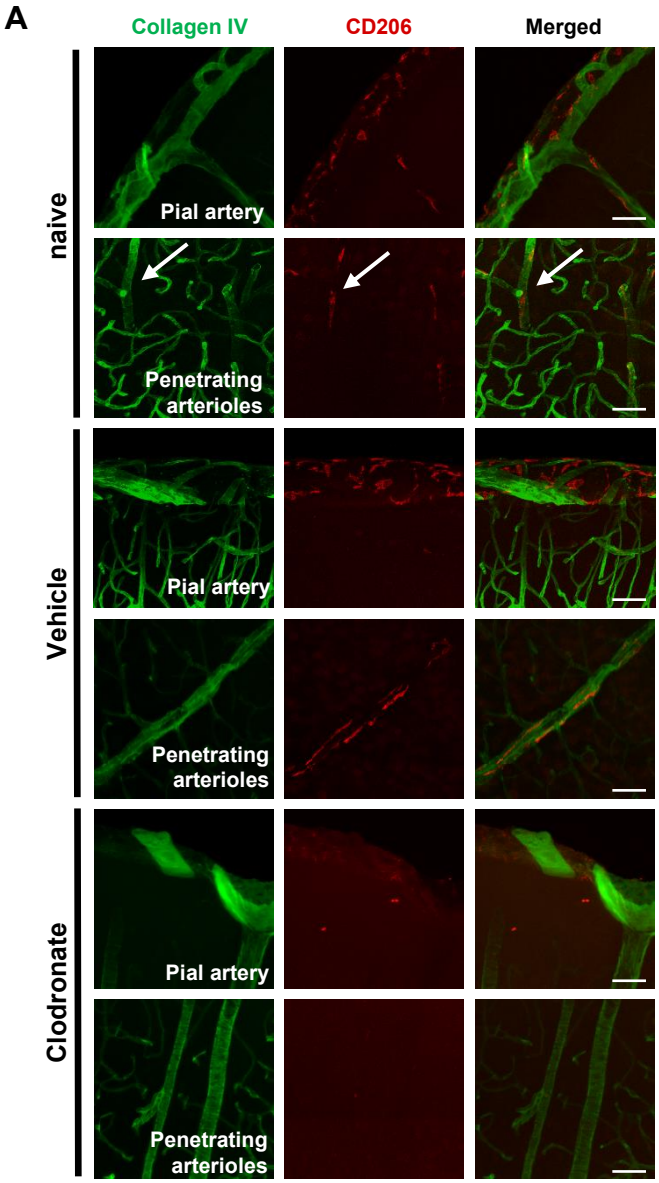
A
Collagen IV
CD206
Merged
naive
Pial artery
Penetrating arterioles
Vehicle
Pial artery
Penetrating arterioles
Clodronate
Pial artery
Penetrating arterioles

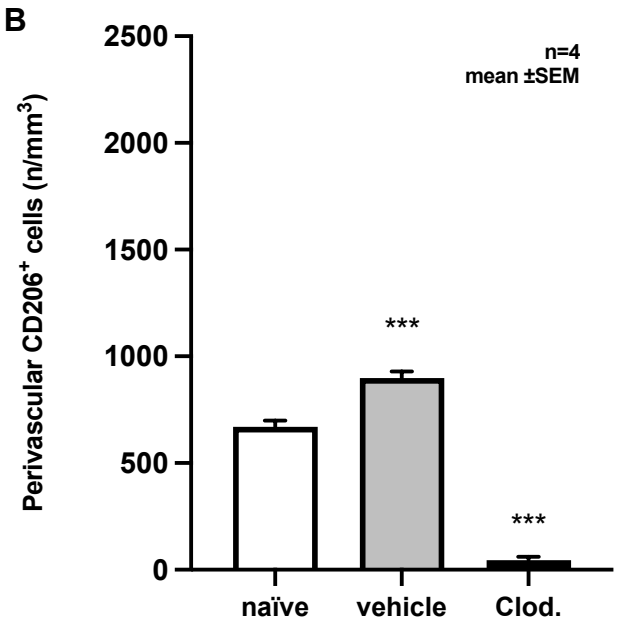
B
Perivascular CD206+ cells (n/mm3)
2500
2000
1500
1000
500
0
n=4
mean ±SEM
***
***
naïve
vehicle
Clod.

Figure 4

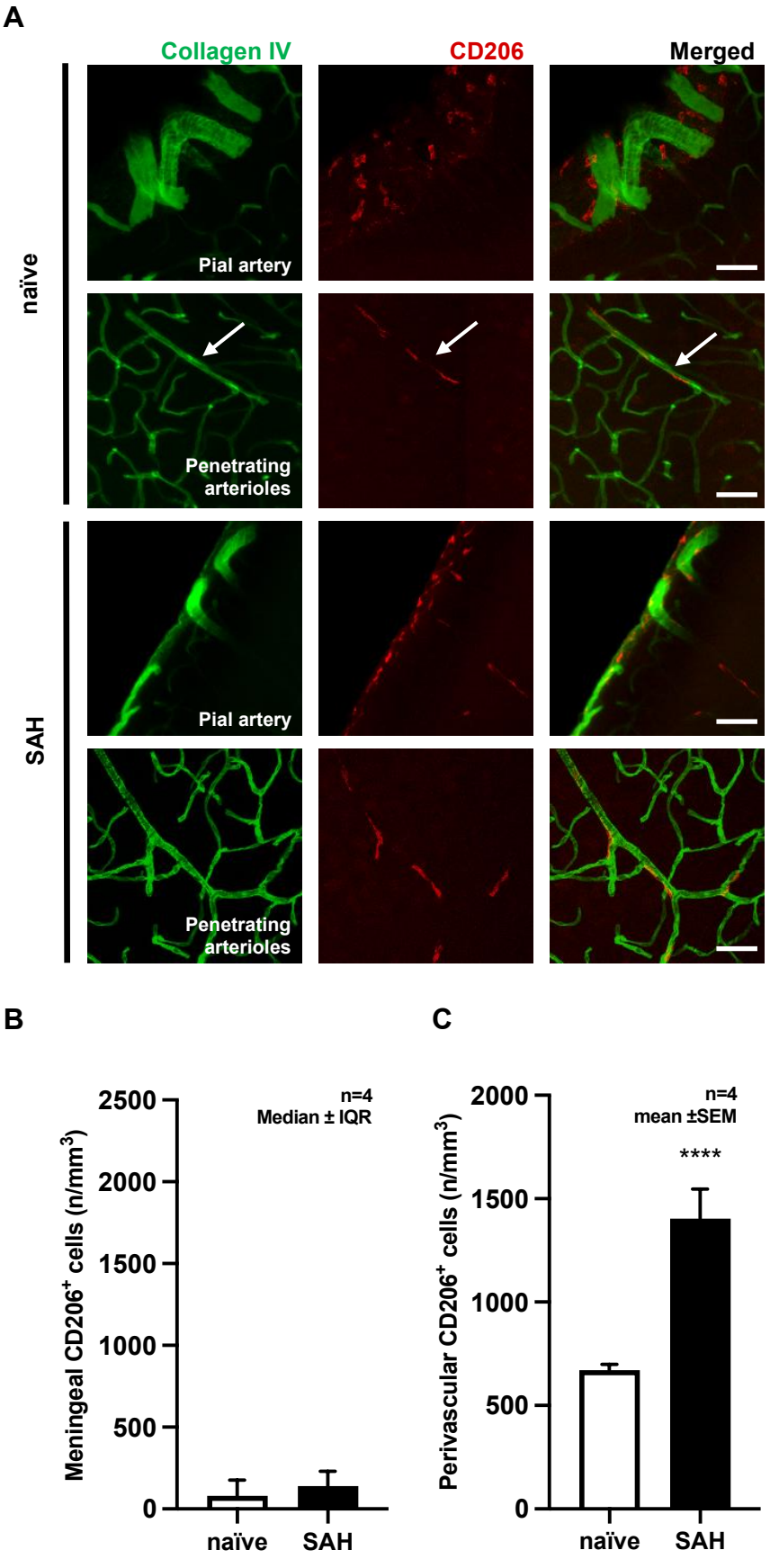
A
Collagen IV
CD206
Merged
naïve
Pial artery
Penetrating arterioles
SAH
Pial artery
Penetrating arterioles
B
n=4
Median ± IQR
Meningeal CD206+ cells (n/mm3)
2500
2000
1500
1000
500
0
naïve
SAH
C
n=4
mean ±SEM
****
Perivascular CD206+ cells (n/mm3)
2000
1500
1000
500
0
naïve
SAH

Figure 5

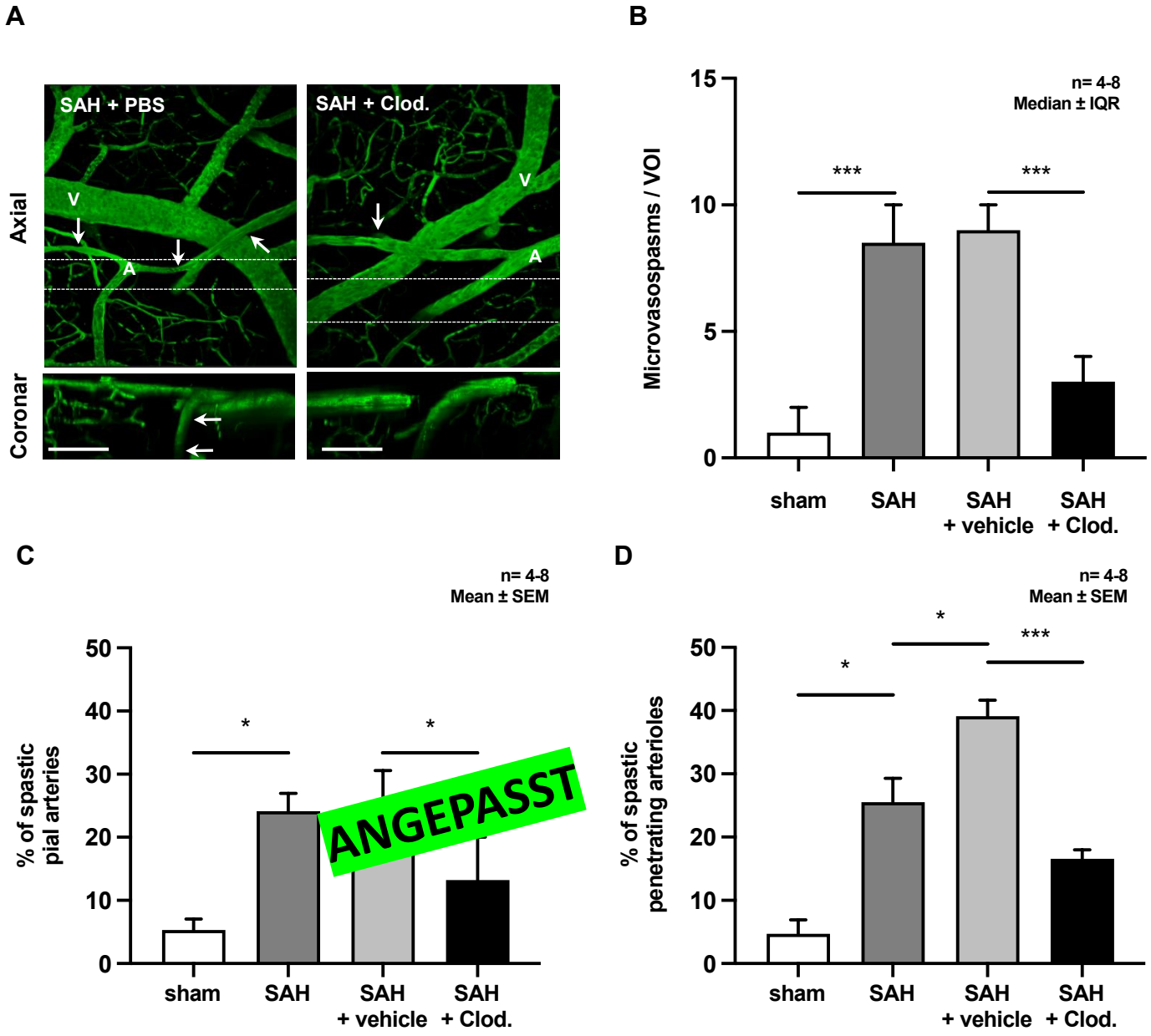
A
SAH + PBS
SAH + Clod.
Axial
Coronar
V
A
B
n= 4-8
Median ± IQR
Microvasospasms / VOI
15
10
5
0
***
***
sham
SAH
SAH + vehicle
SAH + Clod.
C
n= 4-8
Mean ± SEM
% of spastic pial arteries
50
40
30
20
10
0
*
*
ANGEPASST
sham
SAH
SAH + vehicle
SAH + Clod.
D
n= 4-8
Mean ± SEM
% of spastic penetrating arterioles
50
40
30
20
10
0
*
*
***
sham
SAH
SAH + vehicle
SAH + Clod.

ABSTRACT

Subarachnoid hemorrhage (SAH) is characterized by acute and delayed reductions of cerebral blood flow (CBF) caused, among others, by spasms of cerebral arteries and arterioles. Recently, inactivation of perivascular macrophages (PVM) has been demonstrated to improve neurological outcome after experimental SAH, however, the undelaying mechanisms of protection remained unclear. The aim of the current study was therefore to Investigate the role of perivascular macrophages (PVM) in the formation of acute microvasospasms (MVS) after experimental SAH.

PVMs were depleted in male C57BL/6 mice by intracerebroventricular application of Clodronate loaded liposomes. Seven day later SAH was induced by filament perforation under continuous monitoring of CBF and intracranial pressure. Six hours after SAH induction, cerebral microvasospasms (MVS) were investigated in nine standardized regions of interest by *in vivo* 2-photon microscopy. Depletion of PVMs was proven by immunohistochemistry for CD206 together with Collagen IV staining.

PVM were located around pial and intraparenchymal arterioles and were effectively depleted by clodronate (-93%). After SAH, MVS were observed in pial arteries and in penetrating and precapillary arterioles and were accompanied by a significant increase in PVM numbers. PVM depletion significantly reduced the number of MVS by 66%.

Our results suggest that PVM contribute to the formation of microvasospasms after experimental SAH.

INTRODUCTION

Subarachnoid hemorrhage (SAH) is a severe subtype of stroke with a high mortality and morbidity resulting in a high socioeconomic burden. (1-3)

In most cases, an intracranial aneurysm ruptures and bleeds into the subarachnoid space, resulting in a rapid increase of intracranial pressure (ICP) and – subsequently - global ischemia, often fatal within minutes. Although interventional and microsurgical techniques advanced and allow a safe and efficient occlusion of aneurysms to prevent rebleeding, mortality after SAH is high and many patients who survive the initial ictus still suffer from significant morbidity.(1)

Major features associated with adverse outcome after SAH include early and delayed cerebral ischemia.(2) Advanced imaging techniques in patients and after experimental SAH show severe cortical hypoperfusion despite normal cerebral perfusion pressure within hours after aneurysm rupture.(4, 5) Spasms of pial and penetrating arterioles (microvasospasms, MVS) have been demonstrated to be associated with acute cortical hypoperfusion. Options to treat MVS are not available yet, since the mechanisms involved in the formation of MVS are not fully understood.(6-8)

Resident brain macrophages originate from yolk sac progenitors, populate the brain in early development, and have been identified to play a critical role in the maintenance of brain homeostasis.(9) Depending on their anatomical location, macrophages are categorized as perivascular (PVM), associated with pial arteries or penetrating arterioles, or meningeal (MM). PVM have been shown to be a major source of reactive oxygen species (ROS), to mediate neurovascular dysfunction (10), and to be involved in the pathophysiology of such diverse brain diseases as Alzheimer´s disease, multiples sclerosis, CNS infections, and arterial hypertension.(9, 10) Intrathecal injection of clodronate liposomes, which are taken up by brain macrophages and

induce apoptosis, allows to specifically delete this distinct cell population from the brain and to study their role in various disease models. (11)

After SAH, blood released into the subarachnoid space at the skull base enters the perivascular space at the Circle of Willis and redistributes from the initial bleeding site along the branches of the middle cerebral artery to the lateral and apical cerebral cortices.(7) Blood cells degrade within the perivascular space and erythrocyte breakdown products, e.g. heme, free iron, or bilirubin, may either directly damage the adjacent vessel wall or may cause inflammation and the subsequent generation of inflammatory cytokines and free radical species, two processes suggested to cause vasoconstriction.(12, 13) Recently, Wan et al. demonstrated that depletion of PVM after experimental SAH improves neurological outcome and reduces perivascular inflammation.(14) Since, we observed in previous studies that degradation of blood products results in the reduction of MVS, we hypothesize that PVM may be critically involved in the formation of MVS.

In the current study, we therefore used mice depleted of PVMs and visualized pial and penetrating arterioles in vivo by 2-photon microscopy to investigate whether these cells are involved in the formation of MVSs after SAH.

METHODOLOGY

Animals and experimental groups

All procedures on animals, group size calculations, and statistical methods were approved by the Government of Upper Bavaria. The results of the study are reported in accordance with the ARRIVE guidelines. 8–10-week old male C57BL/6 mice (Jackson Laboratory, Bar Harbor, USA) were used for all experiments. We investigated 4 different groups: 1. SAH (n=4) animals without intrathecal injection, 2. Sham (n=4)

operated animals, treated with the same protocol except for middle cerebral artery perforation, 3. SAH+Vehicle (n=8) and 4. SAH+Clodronate (n=8). All experiments were performed in a strictly randomized and blinded manner, i.e. all investigators were unaware of the PVM status of the mice until all experiments were performed and all data was analyzed.

Depletion of perivascular macrophages

Intrathecally injected liposomes loaded with clodronate, a substance which induces apoptosis once taken up by cells, were used to deplete perivascular macrophages (Liposoma, Netherlands) seven days prior to SAH (**Fig. 1A**). Liposomes without clodronate served as vehicle control. For intrathecal injection, animals were anesthetized, fixed in a stereotactic frame (Foehr Medical Instruments, Germany), and the atlanto-occipital membrane covering the cisterna magna was exposed. A custom made glass capillary and a microsyringe pump (World Precision instruments, USA) were used to inject 10 µl of liposomes into the cisterna magna at a rate of 3 µl/min.

Induction of subarachnoid hemorrhage

SAH and sham surgery were performed as previously described (7, 12). Briefly, mice were anesthetized with a mixture of 0.05 mg/kg fentanyl (Janssen-Cilac, Neuss, Germany), 0.5 mg/kg medetomidine (Pfizer, USA) and 5 mg/kg midazolam (Braun, Germany), intubated, and mechanically ventilated. Core body temperature, pO_2, pCO_2, mean arterial blood pressure, oxygen saturation, cerebral blood flow (CBF), and intracranial pressure (ICP) were continuously monitored during surgery. The Circle of Willis was perforated at the outlet of the left middle cerebral artery with an intravascular filament advanced via the common carotid artery. For sham surgery, the filament was inserted and not advanced far enough to induce perforation. Monitoring was continued for 20 minutes after SAH induction. Anesthesia was then antagonized by

subcutaneous injection of 1.2 mg/kg naloxone (Actavis, Ireland, USA), 0.5 mg/kg flumazenil (Inresa, Germany) and 2.5 mg/kg atipamezol (Pfizer, USA).

Two-photon microscopy

In vivo imaging was performed with a LSM 7 microscope (Zeiss, Germany), equipped with a Li:Ti laser (Chameleon, Coherent, USA), 6 hours after SAH/sham surgery (**Fig. 1A**). Animals were anaesthetized as described above and received a femoral artery catheter. A thinned skull window was prepared above the left hemisphere as previously described.(7) Nine random 500 x 500 µm regions of interest (ROI) were imaged to a depth of 250 µm (**Fig. 1B**) 6 h after SAH using a 20x objective (Zeiss, Germany). Animals were continuously monitored for endexpiratory pCO_2, body temperature, heart rate, and peripheral oxygen saturation during imaging. To visualize the microcirculation, 100 µl Fluoresceinisothiocyanate (FITC) dextran (0.5% in saline, Sigma Aldrich, USA) by i.a. injection (G).

Histological analysis and quantification

Mice were perfusion fixed with 4% paraformaldehyde after in-vivo imaging by cardial perfusion and 50 µm free-floating coronal brain sections were collected. Perivascular macrophages were labelled primarily with a $CD206^+$ antibody (BIO-RAD, USA, 1:100). The vasculature was primarily stained with Collagen IV (Abcam, USA, 1:100). As secondary antibodies Donkey Anti-Rat IgG (Abcam, USA, 1:200) and Donkey Anti-Rabbit IgG (**Jackson, USA, 1:200)** were used. Slices were incubated with the primary antibodies for 3 days at 4°C and with the secondary antibodies for 2 days at 4°C. Cell nuclei were labelled by DAPI (1mg/ml, 1:1000, Vector Labs, USA). Perivascular macrophages were defined by positive staining with CD206 and direct contact to a vessel. Meningeal macrophages were defined as $CD206^+$ meningeal cells without vascular contact. Sections were imaged by confocal microscopy (LSM810, Zeiss,

Germany) and six standardized ROIs per animal were analyzed in a randomized and blinded fashion.

In vivo data analysis and quantification

Image analysis was performed with Fiji Image J, Version 2.3. Arteries and arterioles were distinguished from veins by autofluorescence of the vessel wall and blood flow direction. Pial vessels were analyzed in axial planes and penetrating arteries were analyzed in coronal or sagittal planes. Microvasospasms were identified by calculating the constriction grade of the spastic vessel compared with a non-spastic vessel segment as previously described.(15) Microvasospasm was defined as a reduction of the vessel diameter ≥15% compared to a non-spastic vessel segment.

Statistical analysis

Data sets were tested for normal distribution with the D'Agostino & Pearson test and presented as mean ± standard deviation, when normally distributed. Otherwise, medians ± percentiles were used. Statistically significant differences between groups were tested with student´s t tests for parametric data and with the Mann-Whitney test for non-parametric data using Prism 8 (Graphpad Software LLC, USA).

RESULTS

After SAH induction, brain perfusion was globally reduced in all mice. There was no difference between animals receiving Clodronate (Clo) or PBS (**Fig. 1C**). Sham operated animals showed not changes in CBF.

Number of brain macrophages before and after depletion

In naïve C57BL/6 mice, we found 101 ± 14 $CD206^+$ cells/mm^3 without vessel association (meningeal macrophages). Additionally, we also found 671 ± 28 $CD206^+$ cells/mm^3 associated with vessels, i.e. perivascular macrophages (PVMs). PVMs have

an elongated shape and wrap around microvessels (**Fig. 2A**). Most PVMs were located adjacent to pial arteries (276 ± 24 /mm^3); PVM density on intraparenchymal vessels was somewhat lower (precapillary arteries: 238 ± 16 /mm^3 and penetrating arteries; 163 ± 15 / mm^3; **Fig. 2B**), but still 3-5 time higher than the number of meningeal macrophages.

Application of clodronate-loaded liposomes depleted almost all PVM within seven days (**Fig. 3A**). Quantification of the immunohistochemical stainings revealed a reduction of the number of PVM from about 650 PVM/mm^3 in naïve mice, a number well in line with our previous quantification (**Fig. 2B**), to only 46 ± 14 PVM/mm^3 ($p<.001$), i.e. a reduction of about 93%. Interestingly, we also observed a small but significant increase in the number of PVM in vehicle treated mice as compared to naïve animals (Fig. **3B**, $p<.001$) suggesting that an injection with a thin glass capillary through the atlano-occipital membrane was sufficient to induce some PVM proliferation. Since the morphology of the PVM was the same as in unhandled mice (**Fig. 3A**), a major activation of these cells at the time of SAH could be excluded with a sufficiently high degree of confidence.

Number of brain macrophages after SAH

Six hours after SAH, brain macrophages remained unchanged with regard to morphology or distribution as compared to naïve mice (**Fig. 4A**), however, their number increased (**Fig. 4B&C**). While the number of meningeal CD206$^+$ cells increased without reaching statistical significance (**Fig. 4B**, $p=0.07$), the number of PVMs more than doubled after SAH (Fig. **4C**, $p<0.001$). These findings suggest that PVM proliferate particularly rapidly when they come into contact with perivascular blood.

Depletion of perivascular macrophages reduces MVS after SAH

As previously described (7, 12, 16), SAH induces a high number of MVS (**Fig. 5A&B**) in pial and penetrating arterioles (**Fig. 5C&D**). In mice depleted of PVM the number of MVS was reduced by 66% (**Fig. 5A&B;** 9 IQR 5 vs. 3 IQR 3) and the proportion of spastic pial and penetrating arterioles was also reduced (**Fig. 5C&D**). These findings suggest that PVM are critically involved in the formation of MVS.

DISCUSSION

Already in the subacute and acute phase, SAH leads to microvascular constriction and microvasospasm formation which decreases cortical perfusion thereby causing tissue ischemia and subsequent early brain injury.(6-8, 15) PVM were shown to improve outcome after SAH (14), however, it remained unclear how this protective effect was mediated in regard to microvasospasm formation. In the present study, we reproduced previous results from our laboratory that pial and penetrating arterioles constrict acutely after SAH *in vivo* (7, 12, 16), performed the first detailed characterizations of the location and morphology of macrophages in relation to the cortical microcirculation, and confirmed that intrathecal injection of clodronate loaded liposomes depleted more than 90% of PVM. The main finding of the current study is that depletion of PVM reduces early microvasospasm formation to a large degree (-70%). These results suggest that PVM play an important and so far unrecognized role for the formation of microvasospasms after SAH.

All experiments were performed and analyzed in a fully randomized and blinded manner using a clinically relevant SAH model. Since also humans have PVM and a very similar microvascular anatomy as compared to mice(17), we have sufficient evidence to believe that our results are robust and mirror the events which occur also in the human brain after SAH.

Despite the apparent involvement of PVM in MVS formation, the underlying molecular mechanisms need further investigation. The starting point of a cascade of events finally leading to MVS seem to be blood degradation products (18), which already have been demonstrated to negatively impact the cerebral microcirculation after SAH.(12) Within hours after bleeding onset, erythrocytes are phagocytosed and degraded by macrophages as already shown after intracerebral hemorrhage.(19, 20) Alternatively, erythrocytes may also decompose by autolysis.(21) These processes result in the release of blood degradation products, e.g. free iron and hemoglobin, which then accumulate at high concentrations in the narrow perivascular space (18). Free hemoglobin is a very potent nitric oxide (NO) scavenger and may therefore cause local depletion of NO und subsequent vasoconstriction. (22) That this mechanism occurs after SAH is supported by experiments demonstrating that application of NO to cerebral microvessels resolves MVS and improves outcome after experimental SAH.(8, 23) Further, hemoglobin degradation products, e.g. propentdyopents or bilirubin oxidation end products, may directly induce constriction of cerebral microvessels.(24, 25) Another possible and potentially therapeutically relevant way in which PVM could trigger MVS is there activation by blood or blood degradation products and the subsequent release of inflammatory cytokines and free radical species.(17) Free radicals are potent NO scavengers and may, in the end, cause local vasoconstriction. That free radicals do not have a long half-live in living tissues and cannot readily pass cell membranes may explain why MVS have a pearl-string like morphology, i.e. spasms occur only at the site where free radicals are produced by PVM. Further experiments measuring free radical species in spastic microvessels will, however, need to clarify this process in the future.

Despite its apparent advantages, the current study has also some limitations. Clodronate had to be applied by intrathecal injection, however, already the application of vehicle increased the number of $CD206^+$ cells as compared to naive mice. Although these cells had the same morphology as perivascular and meningeal macrophages, we cannot completely rule out that these cells were not blood macrophages which infiltrated the subarachnoid space after injection rather than proliferated PVM. To take the potential influence by blood borne macrophages on our results in to consideration we always used naïve mice as controls for all depletion experiments (where all macrophages were depleted by clodronate treatment).(11)

Another potential limitation is that we performed *in vivo* microscopy through a relatively small cranial window, which allowed us to analyze only a certain fraction of the cerebral cortex. Thus, we cannot generalize our findings to the entire brain.

In conclusion, our results suggest that perivascular macrophages mediate the formation of MVS early after SAH. The underlying mechanism are either the release of free radicals by PVM and subsequent NO scavenging or the degradation of red blood cells by PVM which result in increase of perivascular blood degradation and subsequent NO depletion. Since distinguishing between these two mechanistic pathways may have therapeutic consequences, further studies are needed to fully understand the molecular mechanisms of MVS formation.

Figure Legends

Figure 1

Experimental setup of the experiment

SAH and in vivo imaging performed 7d after intrathecal application of PBS or Clodronate containing Liposomes (**A**). After induction of the SAH, ipsilateral cerebral blood flow (CBF), measured through transcranial laser Doppler probes, was reduced in the SAH groups and the minimal flow was lower after the injection of Clodronate. (**B, left panel**) Contralateral CBF as indirect sign of intracranial pressure was reduced after SAH induction. (**B, right panel**). Imaging was done in 9 standardized volumes of interest (VOI) as shown in (**C**)

Figure 2

Cortical CD206$^+$ macrophages are associated with pial membranes and the microvasculature

Immunohistochemical staining of coronal cuts of the superficial (**A**) and deep (**B**) cortex of naïve 8-10 week old male C57Bl6/n mice with CD206 (macrophages, red) and Collagen IV (microvessels, green). Meningeal Macrophages are CD206$^+$ cells, adjacent to the pial membrane, not associated with vessels (**A**). Perivascular macrophages are CD206$^+$ elongated cells embracing pial arteries, penetrating and precapillary arterioles (**B**). Most CD 206$^+$ cells/ mm^3 are vessel associated (**C**) Scalebar = 20µm.

Figure 3

Intrathecal Liposome injection increases numbers of vessel associated macrophages while Clodronate Liposome injection leads to a macrophage depletion after 7 days.

(**A**) Immunohistochemical staining of coronal cuts of the cortices of naïve 8-10 week old male C57Bl6/n mice (top), 7d after intrathecal injection of PBS (vehicle) liposomes

(middle) and Clodronate liposomes (bottom). Shapes of $CD206^+$ cells do not vary between groups. (**B**) Quantification of vessel associated CD206+ cells shows an increased number after injection of vehicle liposomes and a strong decrease of cell numbers after depletion by clodronate liposomes. Arrow= Penetrating arteriole; Scalebar = 20µm; *** = p<.001

Figure 4

The number of cortical $CD206^+$ macrophages is increased 8h after SAH.

(**A**) Immunohistochemical staining of coronal cuts of the cortices of 8–10-week-old male C57Bl6/n mice without (top) or with (bottom) SAH induction. $CD206^+$ Macrophages are labelled red and Collagen IV^+ microvessels are labelled green. Quantification shows a trend towards increasing numbers of meninges associated $CD206^+$ cells without direct vessel contact (**B**) and significantly more vessel associated $CD206^+$ cells (**C**) after SAH. Arrow= Penetrating arteriole; Scalebar = 20µm, *** = p<.001

Figure 5

PVM depletion reduces microarterial constriction and microvasospasm formation after SAH.

(**A**) Exemplary intravital microscopy images in axial (upper row) and coronal (lower row) projection. High resolution axial and coronal in-vivo 2 photon microscopy 6h after SAH in C57Bl6/n mice with intraarterial labelling 7d after intrathecal injection of Liposomes containing PBS(left image) or Clodronate(right image). Arrows label pearlstring shaped spasms in pial arteries and penetrating arterioles labelled with A, Veins are labelled with V. Dashed Lines show the Location of the maximum intensity projection of the coronal image shown below. Scalebar = 100µm

(**B**) Median number ± IQR of microvasospasms in the observed VOI. Percentage of spastic/ constricted vessels in the examined volume of interest in pial (**C**) and (**D**) penetrating vessels shown as mean ± SEM.

** = p<.01, *** = p < .001

Conflicts of Interest

None.

Acknowledgments

We would like to thank Uta Mamrak for excellent technical and organizational support.

Funding Sources

This project was supported by the “Fakultätsförderprogramm für Forschung und Lehre” (FöFoLe; project #1075) to JS by the Medical Faculty of the University of Munich and by the Deutsche Forschungsgemeinschaft (DFG, German Research Foundation) under Germany’s Excellence Strategy within the framework of the Munich Cluster for Systems Neurology (EXC 2145 SyNergy – ID 390857198).

1. Hoogmoed J, de Oliveira Manoel AL, Coert BA, Marotta TR, Macdonald RL, Vandertop WP, et al. Why Do Patients with Poor-Grade Subarachnoid Hemorrhage Die? World Neurosurg. 2019;131:e508-e13.
2. Macdonald RL, Schweizer TA. Spontaneous subarachnoid haemorrhage. Lancet. 2017;389(10069):655-66.
3. Neifert SN, Chapman EK, Martini ML, Shuman WH, Schupper AJ, Oermann EK, et al. Aneurysmal Subarachnoid Hemorrhage: the Last Decade. Transl Stroke Res. 2021;12(3):428-46.
4. Schubert GA, Seiz M, Hegewald AA, Manville J, Thome C. Acute hypoperfusion immediately after subarachnoid hemorrhage: a xenon contrast-enhanced CT study. J Neurotrauma. 2009;26(12):2225-31.
5. Schubert GA, Seiz M, Hegewald AA, Manville J, Thome C. Hypoperfusion in the acute phase of subarachnoid hemorrhage. Acta neurochirurgica Supplement. 2011;110(Pt 1):35-8.
6. Liu H, Dienel A, Scholler K, Schwarzmaier SM, Nehrkorn K, Plesnila N, et al. Microvasospasms After Experimental Subarachnoid Hemorrhage Do Not Depend on Endothelin A Receptors. Stroke. 2018;49(3):693-9.
7. Schwarting J, Nehrkorn K, Liu H, Plesnila N, Terpolilli NA. Role of Pial Microvasospasms and Leukocyte Plugging for Parenchymal Perfusion after Subarachnoid Hemorrhage Assessed by In Vivo Multi-Photon Microscopy. Int J Mol Sci. 2021;22(16).
8. Terpolilli NA, Brem C, Buhler D, Plesnila N. Are We Barking Up the Wrong Vessels? Cerebral Microcirculation After Subarachnoid Hemorrhage. Stroke. 2015;46(10):3014-9.
9. Faraco G, Park L, Anrather J, Iadecola C. Brain perivascular macrophages: characterization and functional roles in health and disease. J Mol Med (Berl). 2017;95(11):1143-52.
10. Santisteban MM, Iadecola C. Hypertension, dietary salt and cognitive impairment. J Cereb Blood Flow Metab. 2018;38(12):2112-28.
11. Polfliet MM, Goede PH, van Kesteren-Hendrikx EM, van Rooijen N, Dijkstra CD, van den Berg TK. A method for the selective depletion of perivascular and meningeal macrophages in the central nervous system. J Neuroimmunol. 2001;116(2):188-95.
12. Liu H, Schwarting J, Terpolilli NA, Nehrkorn K, Plesnila N. Scavenging Free Iron Reduces Arteriolar Microvasospasms After Experimental Subarachnoid Hemorrhage. Stroke. 2021;52(12):4033-42.
13. Weiland J, Beez A, Westermaier T, Kunze E, Siren AL, Lilla N. Neuroprotective Strategies in Aneurysmal Subarachnoid Hemorrhage (aSAH). Int J Mol Sci. 2021;22(11).
14. Wan H, Brathwaite S, Ai J, Hynynen K, Macdonald RL. Role of perivascular and meningeal macrophages in outcome following experimental subarachnoid hemorrhage. J Cereb Blood Flow Metab. 2021:271678X20980296.
15. Lenz IJ, Plesnila N, Terpolilli NA. Role of endothelial nitric oxide synthase for early brain injury after subarachnoid hemorrhage in mice. J Cereb Blood Flow Metab. 2020:271678X20973787.
16. Friedrich B, Muller F, Feiler S, Scholler K, Plesnila N. Experimental subarachnoid hemorrhage causes early and long-lasting microarterial constriction and microthrombosis: an in-vivo microscopy study. J Cereb Blood Flow Metab. 2012;32(3):447-55.
17. Lapenna A, De Palma M, Lewis CE. Perivascular macrophages in health and disease. Nat Rev Immunol. 2018;18(11):689-702.
18. Plesnila N. Are We Looking Into an Iron Age for Subarachnoid Hemorrhage? Stroke. 2022:STROKEAHA121037670.
19. Zhao X, Grotta J, Gonzales N, Aronowski J. Hematoma resolution as a therapeutic target: the role of microglia/macrophages. Stroke. 2009;40(3 Suppl):S92-4.
20. Chang CF, Massey J, Osherov A, Angenendt da Costa LH, Sansing LH. Bexarotene Enhances Macrophage Erythrophagocytosis and Hematoma Clearance in Experimental Intracerebral Hemorrhage. Stroke. 2020;51(2):612-8.
21. Peterson JW, Roussos L, Kwun BD, Hackett JD, Owen CJ, Zervas NT. Evidence of the role of hemolysis in experimental cerebral vasospasm. J Neurosurg. 1990;72(5):775-81.
22. Hugelshofer M, Buzzi RM, Schaer CA, Richter H, Akeret K, Anagnostakou V, et al. Haptoglobin administration into the subarachnoid space prevents hemoglobin-induced cerebral vasospasm. J Clin Invest. 2019;129(12):5219-35.
23. Terpolilli NA, Feiler S, Dienel A, Muller F, Heumos N, Friedrich B, et al. Nitric oxide inhalation reduces brain damage, prevents mortality, and improves neurological outcome after subarachnoid hemorrhage by resolving early pial microvasospasms. J Cereb Blood Flow Metab. 2016;36(12):2096-107.

24. Joerk A, Ritter M, Langguth N, Seidel RA, Freitag D, Herrmann KH, et al. Propentdyopents as Heme Degradation Intermediates Constrict Mouse Cerebral Arterioles and Are Present in the Cerebrospinal Fluid of Patients With Subarachnoid Hemorrhage. Circ Res. 2019;124(12):e101-e14.
25. Fumoto T, Naraoka M, Katagai T, Li Y, Shimamura N, Ohkuma H. The Role of Oxidative Stress in Microvascular Disturbances after Experimental Subarachnoid Hemorrhage. Transl Stroke Res. 2019;10(6):684-94.